

AD-A209 703

NUMERICAL SIMULATION OF
SUPERSONIC FREE SHEAR LAYERS

Office of Naval Research Contract N00014-89-J1319

Attn: Dr. S. G. Lekoudis

Semi-Annual Progress Report

For the Period

Dec 1, 1988 - May 31, 1989

Prepared by

L. N. Sankar
Associate Professor

Wei Tang
Research Engineer

School of Aerospace Engineering
Georgia Institute of Technology, Atlanta, GA 30332

DTIC
ELECTE
JUN 22 1989
S D

DISTRIBUTION STATEMENT A
Approved for public release;
Distribution Unlimited

88 14

INTRODUCTION

The objective of the present research is to investigate the stability and growth characteristics of 2-D and 3-D supersonic free shear layers through direct numerical solution of the 3-D compressible viscous flow equations.

An explicit time marching method, patterned after the well known MacCormack scheme is used to integrate the 2-D and 3-D Navier-Stokes equations in time, on a stretched Cartesian grid. The flow being studied consists of shear layers formed at the juncture of two parallel streams at different Mach numbers, densities and temperatures. Assuming an initial velocity, density and temperature distribution at an upstream location, the mean steady flow characteristics of the shear layer are first computed. This is done by marching in time, until an asymptotically steady state solution for the mean flow is obtained. Next, acoustic disturbances composed of streamwise, normal or spanwise sinusoidal velocity perturbations at known frequencies are imposed on the shear layer. The limit cycle behavior of the shear layer is then computed by carrying out the calculations for several cycles of the imposed disturbance.

The computed flow field properties are post-processed using standard graphics techniques to obtain vorticity, pressure and density plots, velocity and Mach numbers of eddies, the Fourier spectrum of the velocity and pressure field at a number of locations within the shear layer and so on. Based on the post processing, quantitative conclusions, listed in the next section, are drawn.

The calculations were done on a Cray XMP system installed at the Pittsburgh Supercomputer Center. Computer time for the calculations was provided by NSF under a grant.

Accession For		
NTIS	CRA&I	<input checked="" type="checkbox"/>
DTIC	TAB	<input type="checkbox"/>
Unannounced		<input type="checkbox"/>
Justification		
By <i>AT</i>		
Distribution		
Availability Codes		
Distribution Statement		
<i>A-1</i>		

SUMMARY OF SIGNIFICANT RESULTS

In the appendix, three recent publications are enclosed, describing the solution procedure and significant computed results to date [Ref.1-3]. Here, the conclusions of the present research to date are listed:

1. The shear layer growth rate decreases with increase in the convective Mach number of the eddies.

2. The eddies generated in the shear layer as a result of the acoustic disturbances appear to travel at a velocity closer to the faster stream.

3. When the relative Mach number of the eddies with respect to one or both the streams is sufficiently high, shocklets are formed in the shear layer. Its role on the reduction in the shear layer growth rate is likely to be small.

4. When the shear layer is excited at multiple frequencies, eddies form in response to the excitation. Several of these eddies eventually merge together to form a larger, stronger vortex as they are convected downstream. In the Fourier transform of the pressures at several x- stations, this vortex merging leads to a shift in the energy content from the high frequencies to the low frequencies.

APPENDIX

The appendix consists of the following publications:

1. Tang, W., Komerath, N. and Sankar, L. N., "Numerical Simulation of the Growth of Eddies in Supersonic Free Shear Layers," AIAA paper 89-0376, 1989. To appear in Journal of Propulsion and Power.

2. Tang, W., Sankar, L.N. and Komerath, N., "Mixing Enhancement in Supersonic Free Shear Layers," AIAA Paper 89-0981, March 1989.

3. Sankar, L. N. and Tang, W., Proceedings of the AFOSR/ONR Contractors Meeting, Ann Arbor, Michigan, June 19-22, 1989.

Presented at the AFOSR/ONR Contractors
Meeting, Ann Arbor, Michigan, June 22, 1989

NUMERICAL SIMULATION OF CONTROL OF SUPERSONIC SHEAR LAYERS

ONR Contract No. N00014-89-J-1319

Principal Investigator: L. N. Sankar

School of Aerospace Engineering
Georgia Institute of Technology, Atlanta, GA 30332

SUMMARY

The issue of enhancing mixing between parallel, supersonic streams is numerically investigated. An explicit time marching scheme that is second order accurate in time and fourth order accurate in space is used to study this problem. Small amplitude velocity disturbances at selected frequencies are imposed over an otherwise steady flow at the juncture of the two streams to promote mixing. It is found that disturbances are selectively amplified at certain frequencies, while disturbances at other frequencies are rapidly damped out. In studies where the relative Mach number of the disturbances relative to one of the streams is high, shocklets were found to form on one or both sides of the shear layers. In such a situation, the relative Mach numbers of the eddies were different in coordinate systems attached to the upper and the lower streams.

SCOPE OF THE PRESENT WORK

The objectives of the present work are to study the growth of supersonic free shear layers and their response to imposed acoustic disturbances through direct numerical solution of the governing equations.

The 2-D compressible Navier-Stokes equations in a strong conservation form are numerically solved, using a modified MacCormack scheme that is second order accurate in time, and fourth order accurate in space. This scheme is suitable for studying phenomena such as propagation of acoustic waves, boundary layer instability, and shear layer instability and has been previously used by several authors. The flow field is assumed to be laminar.

RESULTS AND DISCUSSION

Figure 1 shows the computational domain used. The computational domain was divided into a uniformly spaced Cartesian grid consisting of 221 nodes in the x- direction and 241 nodes in the normal direction. The typical grid spacing in the x- and y- direction were $5/3d$ and $0.4 d$ units respectively, where d is the vorticity thickness of the shear layer at the inflow boundary. The grid spacing in the y- direction is fine enough to place approximately 30 points across the shear layer where the vorticity content is largest, at distances sufficiently downstream ($x > 50d$) from the inlet.

At the inflow boundary, a hyperbolic tangent mean velocity profile was specified. The v component of inflow velocity was set to zero for the mean flow. The pressure was assumed to be equal and uniform at the inflow boundary. A variety of velocity, density and temperature ratios across the shear layer have been used to study parametrically their effects on the shear layer characteristics.

The 2-D Navier-Stokes solver was used to compute the mean shear flow characteristics first. Then, forced excitation of the shear layer began. This was achieved by prescribing the normal (v -) component of velocity over the entire inflow boundary to behave as follows:

$$v(y, x=0, t) = \sum A_n f(y) \sin(x_n t + \theta_n)$$

Here the summation shown is over all the excitation frequencies; A_n is the amplitude of disturbance, x_n is the frequency of disturbance and θ_n is the associated phase angle. The function $f(y)$ determines the variation of the perturbation velocity across the shear layer. Both a Gaussian distribution and a constant magnitude distribution were attempted. The results to be presented here correspond to $f(y)$ equal to unity.

The computed flow fields after several cycles of forced excitation of the shear layer are analyzed using computer graphics and Fourier transform techniques to study the following issues of interest:

- a) Effect of convective Mach number on shear layer growth
- b) Correlation between computed convective Mach number of eddies and analytical estimates
- c) Occurrence of shocklets and their effects on shear layer growth
- d) The growth and decay of low and high frequency excitations with time and space.

The following conclusions were drawn:

a) In the case of shear layers at subsonic and supersonic convective Mach numbers, the imposition of acoustic disturbances over a large range of frequencies lead to the transfer of this energy from the high frequencies to the low frequencies, as the flow progressed from the upstream boundary to the downstream boundary. The energy content at the lowermost frequencies rapidly reached asymptotic values following which eddies in the shear layer were convected downstream with no further alteration in their structure [Figure 2].

b) In the case of shear layers at a supersonic convective Mach number, situations were found where the convective Mach number relative to the faster stream is low. This leads to a situation where shocklets arose only on the lower side of the shear layer. Conditions were also found where the convective Mach number relative to both the streams is high, leading to shocklets on either side [e.g. Figure 3]. These calculations demonstrate the same features

experimentally observed by Papamoschou and discussed based on total pressure arguments by Dimotakis.

c) The spatial growth of shear layers decreased with increasing convective Mach number.

ACKNOWLEDGEMENTS

This work was supported by the Office of Naval Research under Grant No. N00014-89-J-1319. Computer time for the numerical simulations was provided by the Pittsburgh Supercomputing Center. The authors are thankful to Prof. S. A. Ragab of Virginia Polytechnic Institute & State University for several valuable discussions.

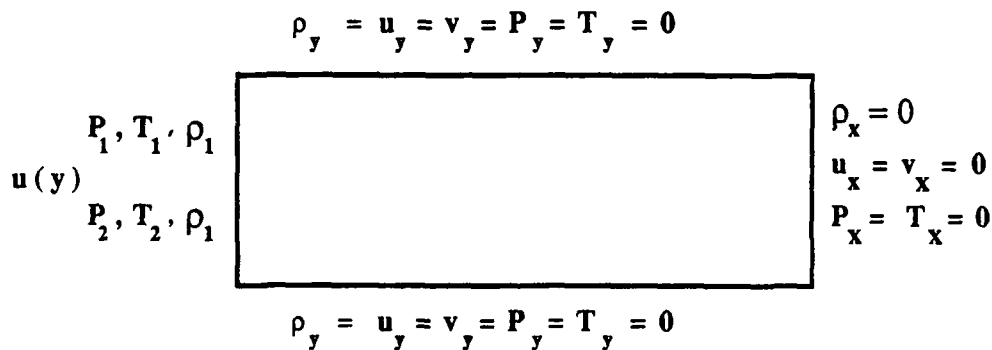
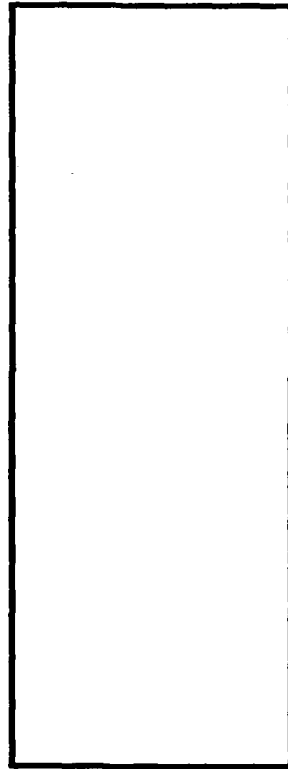


Fig. 1 Computational Domain and Boundary Conditions

COMPUTATIONAL DOMAIN AND BOUNDARY CONDITIONS

$$\rho_y = u_y = v_y = P_y = T_y = 0$$



$$\begin{aligned} \rho_x &= 0 \\ u_x &= v_x = 0 \\ P_x &= T_x = 0 \end{aligned}$$

$$\begin{aligned} &P_1, T_1, \rho_1 \\ u(y) & \\ &P_2, T_2, \rho_1 \end{aligned}$$

$$\rho_y = u_y = v_y = P_y = T_y = 0$$

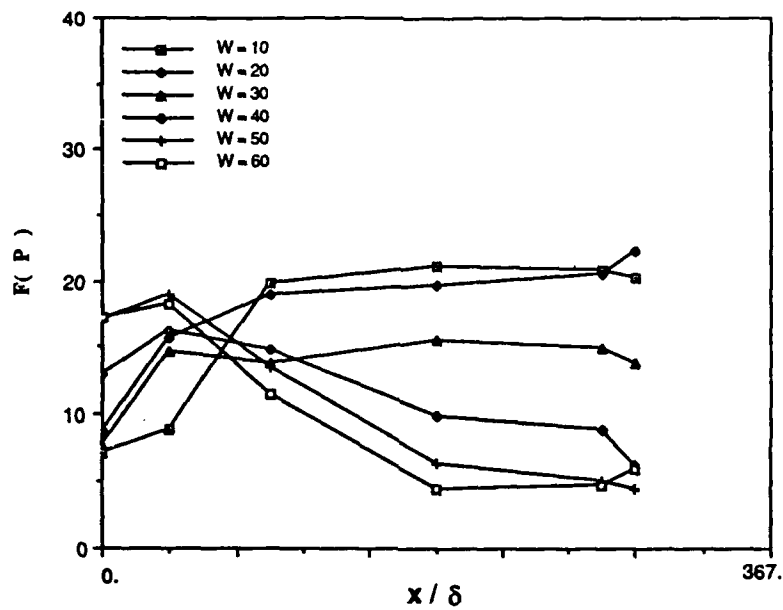


Fig. 2 Variation of Fourier Spectrum

$M_c = 0.2$, $M_1 = 4.0$, $M_2 = 2.3$, $a_1/a_2 = 2.3$, $\delta = 1/15$, Multi-Frequency

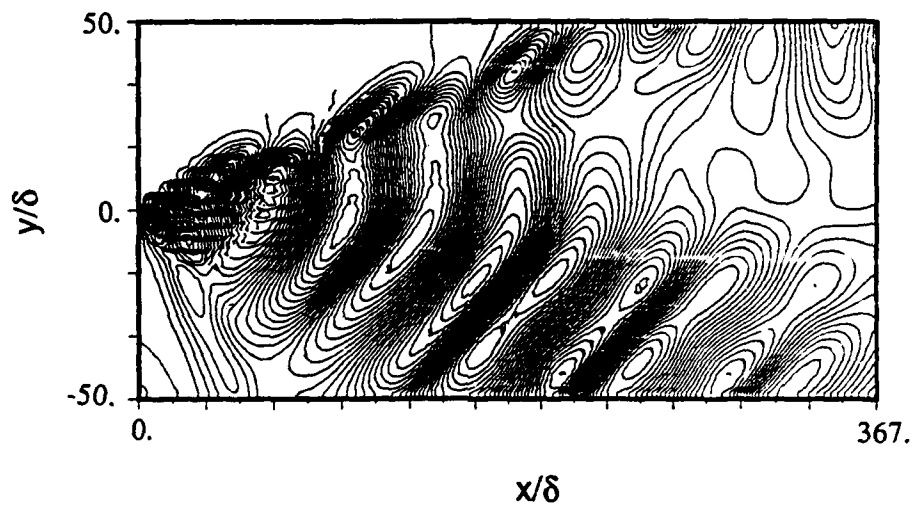


Fig. 3 Pressure Countours

$M_c = 1.2$, $M_1 = 5.0$, $M_2 = 1.3$, $a_1/a_2 = 2.3$, $\delta = 1.0$

AIAA '89

AIAA 89-0376

**Numerical Simulation of the Growth of
Instabilities in Supersonic Free Shear Layers**

W. Tang, N. Komerath and L. Sankar, Georgia
Institute of Technology, Atlanta, GA

27th Aerospace Sciences Meeting

January 9-12, 1989/Reno, Nevada

NUMERICAL SIMULATION OF THE GROWTH OF INSTABILITIES IN SUPERSONIC FREE SHEAR LAYERS

Wei Tang¹, Narayanan Komerath², and Lakshmi N. Sankar³
School of Aerospace Engineering
Georgia Institute of Technology
Atlanta, Georgia 30332

ABSTRACT

The behavior of the initial region of a supersonic plane shear layer is analyzed through numerical solution of the 2-D Navier-Stokes equations, as well as the 3-D equations under the infinite span assumption. Two schemes are employed and compared: a 2nd order ADI procedure, as well as a modified McCormack scheme that is fourth order accurate in space and second order in time. Small amplitude oscillations in the normal velocity are found to grow as they convect downstream, and eventually lead to organized vortical structures. Normal velocity disturbances are found to be more efficient than streamwise or spanwise disturbances. The growth rate of these disturbances, as well as the intensity of velocity fluctuations, are found to decrease as the convective Mach number of the shear layer increases. The Mach number of the vortical structures with respect to the faster stream are found to be considerably less than the theoretical value of the convective Mach number.

INTRODUCTION

Air-breathing engines designed for high flight Mach numbers require supersonic combustion for efficient operation. The shock losses associated with deceleration to low Mach numbers requires that the mixing of fuel and air, and the heat release, must occur in supersonic flows. For the same reason, it is desirable to mix the fuel and air using co-flowing streams. In such configurations, the mixing must occur across the shear layer formed between the streams. The length and weight of the engine, and the efficiency of heat release, depend on the rapidity of this mixing process. Most current concepts for supersonic-combustion ramjets thus

employ mixing-limited heat release. The mixing across a shear layer between two streams depends on the rate of mass and momentum transfer across the layer, and hence can be described using the "growth" or "spreading" rate of the shear layer. Unfortunately, shear layers separating supersonic streams are known to grow much slower than corresponding subsonic shear layers.

One long-term objective of supersonic shear layer research, therefore, is to devise methods of increasing the mixing between supersonic streams by enhancing the shear layer growth rate. Recent success in greatly modifying subsonic shear layers has resulted in the advancement of a variety of schemes for achieving similar increases in supersonic shear layers. The variety of such possibilities far exceeds the resources available for experimental exploration of each. Instead, a better approach appears to be to develop reliable numerical models and solution methods that can then be used to perform the exploration, and to identify promising approaches and the appropriate values of parameters required. This is the motivation behind the research described in this paper.

Previous Work

Chinzei et al¹ conducted experiments on planar shear layer configurations and studied the growth rate. Papamoschou² conducted similar experiments using a variety of gases and flow conditions and showed that the results could be scaled using the convective Mach number of the dominant eddies in the shear layer. These results showed that the growth rate of supersonic shear layers is typically less than 1/3 the growth rate of incompressible shear layers.

Passive and active control techniques have been studied by other researchers. These techniques are generally based on the principle

1. Research Engineer II. Member, AIAA.
2. Assistant Professor. Member, AIAA.
3. Associate Professor. Member, AIAA.

Copyright ©American Institute of Aeronautics and Astronautics, Inc., 1989. All rights reserved.

that if vorticity is introduced into the shear layer, it will increase the level of fluctuation and therefore promote mixing and growth. Guirguis³ and Drummond et al⁴ studied the effect of a bluff body placed in the middle of the shear layer. Kumar⁵ considered the effects of vorticity produced by a pulsating shock wave on the growth characteristics of the shear layer. Ragab et al⁶ have developed calculations based on stability theory to predict the response of supersonic shear layers. Recently⁷ they have also developed computations of the response of planar wakes and shear layers similar to those in experimental splitter plate configurations.

Scope of Present Paper

In the work presented here, the behavior of a planar free shear layer is studied using two numerical techniques for solution of the Navier-Stokes equations. The effects of active control strategies are investigated. Sinusoidal variations in the velocity are introduced at the upstream boundary. The subsequent response of the shear layer to these disturbances is studied. Streamwise, normal, and spanwise disturbances are considered as suitable candidates for promoting mixing.

At present, the problem is assumed to be nominally two-dimensional. Some calculations have been performed with 3-D layers under the infinite sweep assumption. It is recognized that the later development of the shear layer may be strongly influenced by three-dimensional effects. However, there is no reason to believe that the initial region should be anything other than two-dimensional. The available experimental flow visualizations, performed with spanwise-integrating techniques such as schlieren and shadowgraphy, clearly show structures that would have been totally smeared out if the flowfields had been significantly three-dimensional.

No turbulence model is used. Turbulence models inherently bring additional uncertainty into the physical interpretation of the observed behavior of the flowfield, though they are certainly necessary to obtain quantitative accuracy. The lack of such a model restricts the applicability of these results to the initial region of the shear layer.

The initial velocity profile used is a step change in velocity at the slip line between the two streams. Thus, the results obtained will not correspond to experimental results from splitter-plate configurations, since there is no boundary

layer, and no embedded region of initially subsonic flow.

Within the above limitations, the present work aims to study the behavior of the initial region of a shear layer, and to explore the effects of various forms of excitation.

PROBLEM STATEMENT

The shear layer configuration is shown in Fig. 1. Two uniform, parallel supersonic streams of different Mach numbers are released at the left-hand boundary. All properties are known at this boundary. The upper and lower boundaries of the computational domain are assumed to be hard walls across which no disturbances can escape. There is no boundary layer at these walls, and slip conditions are used. At the downstream boundary, the flow and all disturbances are allowed to escape, and no disturbances are allowed to propagate back.

To study shear layer behavior, the static pressures are equalized across the splitter plate, so that there are no strong shocks in the flow. Some waves and their reflections from the wall do occur, but these are quite weak.

The flow is assumed to be non-reacting, and the ratio of specific heats was assumed to be constant for both streams. The species above and below the shear layer were assumed to have the same molecular weight.

Mathematical Formulation: 4th order McCormack Scheme

$$q_t + F_x + G_y = R_x + S_y$$

Here F and G are the inviscid flux terms and account for the transport of mass moment and energy, and for the influence of pressure. The terms R and S are the viscous stress terms. The above set of equations are parabolic with respect to time, and may be solved using a variety of stable time marching schemes. For 2-D flows there are four equations. In the case of 3-D flows subject to infinite-sweep assumption, there are five equations, the additional equation corresponding to the conservation of spanwise momentum.

In this work the above equation was solved using a splitting approach. That is, the solution was advanced from one time level 'n' to the next 'n+2' through the following sequence of operations

$$q^{n+2} = (L_x L_y L_{xv} L_{yv} L_{yv} L_{xv} L_y L_x) q^n$$

where, for example, the L_x operator involves solution of the following 1-D equation:

$$q_t + F_x = 0$$

This 1-D equation was solved through the following predictor-corrector sequence, recommended by Bayliss et al. [Ref. 7]:

Predictor Step:

$$q_{i,j}^* = q_{i,j}^n - \frac{\Delta t}{6\Delta x} \left[7 F_{i,j} - 8 F_{i-1,j} + F_{i-2,j} \right]^n$$

Corrector Step:

$$q_{i,j}^{n+1} = \frac{1}{2} (q_{i,j}^n + q_{i,j}^*) + \frac{\Delta t}{12\Delta x} \left[7 F_{i,j} - 8 F_{i+1,j} + F_{i+2,j} \right]^*$$

When the above equations are applied at nodes close to the left and right side boundary, a fourth order accurate extrapolation procedure was used to extrapolate the flux vectors F and F^* needed at nodes outside the computational domain.

The L_y operator requires solution of the equation

$$q_t + G_y = 0$$

using a similar approach.

The operators L_{xv} and L_{yv} correspond to numerical solution of 1-D equations such as

$$q_t - R_x = 0$$

The above equation was solved through the following two-step sequence:

$$q_{i,j}^* = q_{i,j}^n + \frac{\Delta t}{\Delta x} \left[R_{i+\frac{1}{2},j} - R_{i-\frac{1}{2},j} \right]^n$$

$$q_{i,j}^{n+1} = \frac{1}{2} (q_{i,j}^n + q_{i,j}^*) + \frac{\Delta t}{2\Delta x} \left[R_{i+\frac{1}{2},j} - R_{i-\frac{1}{2},j} \right]^*$$

The viscous terms are thus updated only to second order accuracy in space. It may be shown that the above scheme has very little artificial dissipation inherent in it, and is fourth order accurate in space, as far as the inviscid part is concerned.

BOUNDARY CONDITIONS

As stated above, all flow properties are prescribed at the upstream boundary for both streams, including any imposed perturbations. At the downstream boundary, the flow is assumed to remain fully supersonic for the small-amplitude perturbations encountered in this work, so that the properties may be extrapolated from the interior. Alternatively, the governing equations themselves may be applied if the streamwise diffusion terms R_x are suppressed at the downstream nodes.

At the lateral boundaries, the flow is assumed to be confined by smooth, parallel walls. Slip boundary conditions were used to avoid the compression effects that would be caused by boundary layers. The walls were considered adiabatic, and the normal derivatives of density and pressure were set to zero.

RESULTS AND DISCUSSION

Normalization

The speed of sound in the upper stream was assumed to be unity. The Reynolds number based on the speed of sound was assumed to be 1000. A 221×61 uniform grid was used, with spacing of .01 in each direction. Thus the length of the domain, L was 2.2. The time step was taken as .001 (.0005 for each half-step). The calculations were started with step velocity profiles at the upstream boundary, and allowed to proceed until a steady state was reached asymptotically. This usually took 600 time steps. The results at this stage were stored, and the code was re-started with an imposed sinusoidal velocity disturbance of amplitude 2% of the velocity of the upper stream. The calculations were then run until several cycles of the disturbance had been completed, and the initial effects had been convected away through the downstream boundary.

Convective Mach Number

The cases run have been summarized in Table 1. Because the supersonic shear flow problem involves several parameters, (at least five on either side of the shear layer), non-dimensional groupings are sought to express observed effects. Following the practice of

Papamoschou², the convective Mach number was used here. For the problem studied here, the convective Mach number reduces to

$$M_c = \frac{U_1 - U_c}{a_1}$$

where

$$U_c = \frac{a_1 U_2 + a_2 U_1}{a_1 + a_2}$$

The values of M_c calculated by this formula are tabulated. A physical interpretation of the convective Mach number is that it is the Mach number of the dominant large-scale vortical structures with respect to either stream. According to the formula given above, this Mach number is the same with respect to either of the streams. An attempt was made, as discussed later, to determine the convection speed of the vortical structures seen in the computational flow field, and to determine relative Mach numbers from them. The Mach numbers so determined, with respect to the upper, high-speed stream, are also tabulated. It is seen that there is a considerable discrepancy. This is not surprising, and in fact even in subsequent experiments by Papamoschou⁹, similar effects appear to have been observed.

Formation of vortical structures

Figure 2 (a) shows the contours of vorticity in the shear layer, calculated for Case 1, with no disturbance superposed. It is seen that the shear layer grows quickly at the very beginning, and then takes on a smooth profile which grows very little thereafter. It should be remembered that in this calculation, there is no imposed turbulence model. Figure 2(b) shows the effect of imposing a sinusoidal 2% normal velocity disturbance at the upper boundary. Distinct centers of vorticity are seen to develop, and be convected downstream. The shear layer edge now penetrates considerably further into both streams. Careful examination of the contours shows considerable asymmetry and distortion as the structures proceed downstream. The computational domain in this calculation does not extend far enough for these disturbances to grow into the non-linear regime, and hence no "roll-up" can be expected here. The effects of six cycles of the imposed disturbance can be seen, with the sixth just leaving the computational domain.

Figure 3(a) and (b) show the corresponding vorticity contours for Case 2, where the theoretical value of convective Mach number is

nearly twice that of Case 1. The growth rate appears to be less, as expected from the experimental observations of the effect of M_c . This effect is seen further in Figs. 4 and 5, where the convective Mach number according to the formula is 0.8 and 1.2 respectively.

Disturbance type

Other kinds of disturbance were tried, specifically, disturbances in velocity along the streamwise direction for the 2-D shear layer, and disturbances along the spanwise direction using a 3-D model with the infinite sweep assumption. The results are shown in Figs. 6 and 7 respectively, for the case where the convective Mach number is predicted to be 0.2. In each case, the disturbance amplitude is the same. It is seen that these types of disturbances are less efficient than the normal velocity disturbance.

Convective speed based on evolution of vorticity contours

One common way of calculating the convective Mach number is to track the downstream convection of the vorticity contours as a function of time. The results of this effort are shown in Fig. 8 for Case 2. Similar computations were performed for all the cases, and the results are shown in Table 1. It is seen that as the theoretical value of the convective Mach number rises, the measured convective Mach number of the structures with respect to the upper stream vary much less. Of course, this means that the convective Mach number is no longer the same when compared to the two streams. The structures appear to move at a speed that is close to that of the upper, high-speed stream. This is similar to the more recent observations of Papamoschou⁹, where the structures were found, for many cases, to move at speeds close to that of one or the other stream.

Growth rate enhancement

The thickness of the shear layer was computed from the velocity profiles across the shear layer. These profiles are shown later in the paper, where they are used to examine the numerical accuracy of the results. Figure 9 shows the shear layer thickness for unperturbed and perturbed cases for Case 1. The disturbed case shows a significantly greater rate of growth, except near the downstream boundary. However, the increase in growth rate is only on the order of 10 to 15%.

The frequency of the imposed fluctuations was chosen such that about 6 vortical structures could be seen in the computational domain at

one time. The actual frequency involved is higher than the frequency of maximum amplification predicted by linear stability analysis.

The intensity of fluctuation in the shear layer is plotted as a function of downstream distance for three cases with different theoretical convective Mach numbers in Figs. 10. The quantity measured was the root-mean squared fluctuation of the U-component of velocity about the mean, normalized by the mean velocity. It is to be noted that this is not the turbulence intensity, since no attempt has been made to model the turbulence. The fluctuations have their origin in the imposed disturbance, though they may have been selectively amplified by energy exchange with the shear layer. It is seen that the intensity of fluctuations decreases rapidly with increasing convective Mach number. It also appears that the intensity quickly reaches an asymptotic value and does not increase further. In fact, for the higher values of convective Mach number, the intensity appears to peak and then decrease gradually thereafter.

Validation studies

All the above results were generated using the fourth-order MacCormack scheme. The influence of the accuracy of the computation scheme was studied by comparing results obtained using a second-order MacCormack scheme to those obtained with the fourth-order scheme. Velocity profiles across the shear layer were used to examine the results. Fig. 11 shows the comparison for Case 1, however, with a 111×31 grid. The profile was obtained at the station 10% of the domain length downstream of the origin. The results are seen to be quite similar. The agreement is close for profiles at 25 and 50% downstream. However, at $X/L = 0.75$, differences can be clearly seen. The 4th order scheme is seen to resolve spatial details better, as expected. The difference decreased further downstream. It is concluded from these that the second order scheme already shows reasonable accuracy, and that the fourth order results are quite accurate.

The effect of grid size was checked by comparing the above results with those obtained with the 221×61 grid, as shown in Fig. 12. In this case, the difference between 2nd and 4th order codes is negligible for all stations. Thus, it is concluded that with the 221×61 grid, the results are not sensitive to grid size.

Comparison with results using an ADI scheme

Previous calculations for this configuration had been performed using an Alternating-Direction Implicit scheme to solve the governing equations. The formulation of this scheme is discussed in detail in Ref. 10. Vorticity contours for Case 1 are shown in Fig. 13. With this technique, it was found that the disturbances would not grow, or lead to the formation of distinct centers of vorticity, except at extremely high values of the imposed perturbation amplitude. The dissipation inherent in the scheme is excessive for the study of disturbance growth. In addition, it was also found that the explicit MacCormack scheme required much less computer resources than the ADI scheme.

Computational Resources

All calculations reported here were performed on the Cray X-MP at the Pittsburgh Supercomputing Center. The CPU times per time step per grid node were 10 and 24.5 microseconds for the 4th order MacCormack scheme and the ADI scheme respectively using the 221×61 grid.

CONCLUSIONS

A numerical study of the behavior of planar supersonic shear layers has been performed. Different numerical schemes have been tested. Techniques for enhancing the growth rate of the shear layer have been investigated. It is noted from the results that:

1. The 4th order MacCormack scheme accurately simulates the evolution of the imposed disturbances. The results are essentially independent of the spatial order of the scheme with a 221×61 grid with the grid parameters used.
2. The ADI scheme causes too much dissipation and fails to reveal the response of the shear layer to imposed disturbances except at very high disturbance amplitudes.
3. Normal velocity perturbations are found to be more efficient than either streamwise or spanwise velocity perturbations.
4. Imposed sinusoidal disturbances in the normal velocity upstream lead to the formation and growth of vortical structures. The shear layer thickness grows rapidly at first and then the growth rate decreases asymptotically.
5. The root-mean square fluctuation level in the streamwise velocity, and the shear layer growth rate decrease with increasing values of the theoretical convective Mach number of the shear layer.

6. The vortical structures are found to move at different Mach numbers relative to the upper and lower stream, and the relative Mach number appears to be smaller relative to the stream with the higher Mach number.

ACKNOWLEDGEMENTS

This work was supported by the Office of Naval Research under contract No. N00014-87-K-0132. Dr. S.G. Lekoudis was the Technical Monitor. Computer resources were provided by a grant from the Pittsburgh Supercomputing Center.

REFERENCES

1. Chinzei, N., Masuya, G., Komuro, T., Murakami, A., and Kudou, K., "Spreading of Two-Dimensional Supersonic Mixing Layers". *Physics of Fluids*, Vol. 29, No. 5, pp. 1345 - 1347, May 1986.
2. Papamoschou, D., "Experimental Investigation of Heterogeneous Compressible Shear Layers". Ph.D. Dissertation, California Institute of Technology, 1986.
3. Guirguis, R.H., "Mixing Enhancement in Supersonic Shear Layers: III. Effect of Convective Mach Number". AIAA 88-0701, January 1988.
4. Drummond, J.P., and Mukunda, H.S., "A Numerical Study of Mixing Enhancement in Supersonic Reacting Flow Fields". AIAA 88-3260, July 1988.
5. Kumar, A., Bushnell, D.M., and Hussaini, M.Y., "A Mixing Augmentation Technique for Hypervelocity Scramjets". AIAA 87-1882, July 1987.
6. Ragab, S.A., and Wu, J.L., "Instabilities in the Free Shear Layer Formed by Two Supersonic Streams". AIAA 88-0038, 1988.
7. Ragab, S.A., "Instabilities in the Wake / Mixing Layer Region of a Splitter Plate Separating Two Supersonic Streams". AIAA 88-3677-CP, Proceedings of the 1st National Fluid Dynamics Congress, Vol. 2, pp. 1095-1102, July 1988.
8. Bayliss, A., Maestrello, L., Parikh, P., and Turkel, E., "Numerical Simulation of Boundary Layer Excitation by Surface Heating and Cooling". *AIAA Journal*, Vol. 24, No. 7, July 1986.
9. Papamoschou, D., Presentation at the Workshop on the Fluid Dynamics of Compressible Turbulent Shear Layers, Cincinnati, OH, July 1988.
10. Sankar, L.N., Tang, W. and Komerath, N.M., "Numerical Simulation of Supersonic Free Shear Layers," International Conference on Computational Engineering Science, Atlanta, GA, April, 1988.

case	M ₁	M ₂	U ₁	U ₂	M _c Papamoschou's formula	M _{vortex} Present results
1	4.0	2.3	4.00	3.51	0.20	0.2
2	4.0	2.0	4.00	3.05	0.38	0.2
3	4.0	1.3	4.00	1.98	0.80	0.2
4	5.0	1.3	5.00	1.98	1.20	0.6

Table 1. Cases presented.

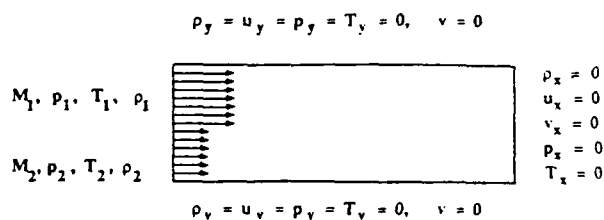


Figure 1. Boundary conditions for supersonic free shear layer.

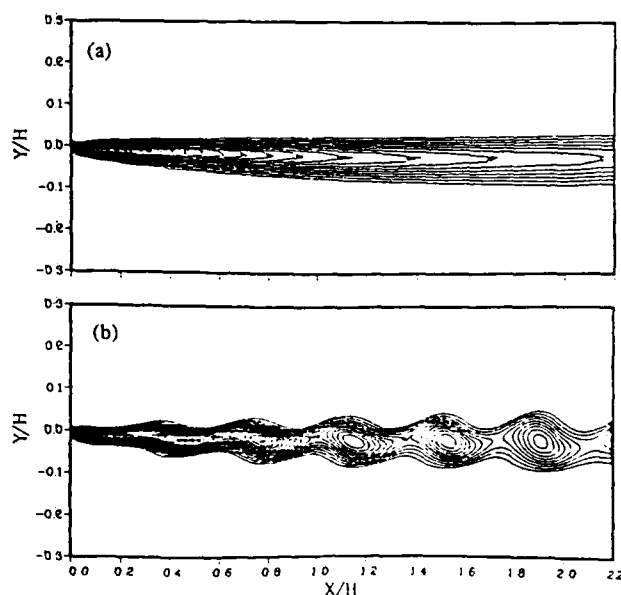


Figure 2. Vorticity contours for case-1, $M_1=4.0$, $M_2=2.3$, $M_c=0.2$. (a) without disturbance. (b) with disturbance in the normal direction.

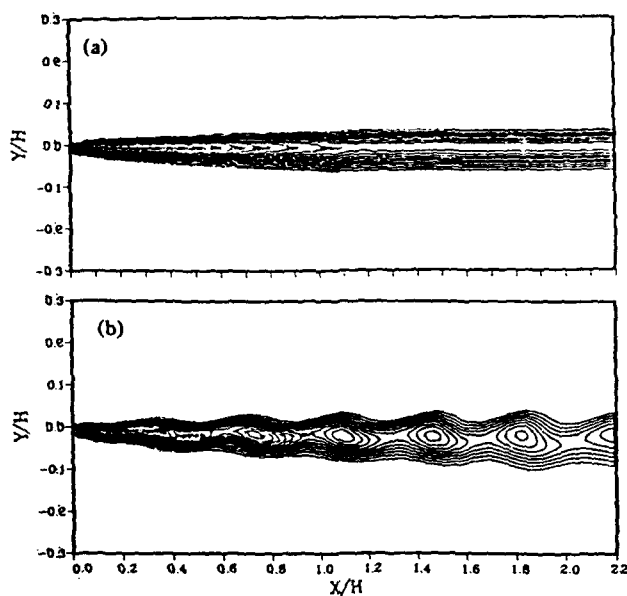


Figure 3. Vorticity contours for case-2, $M_1=4.0$, $M_2=2.0$, $Mc=0.38$.
(a) without disturbance. (b) with disturbance in the normal direction.

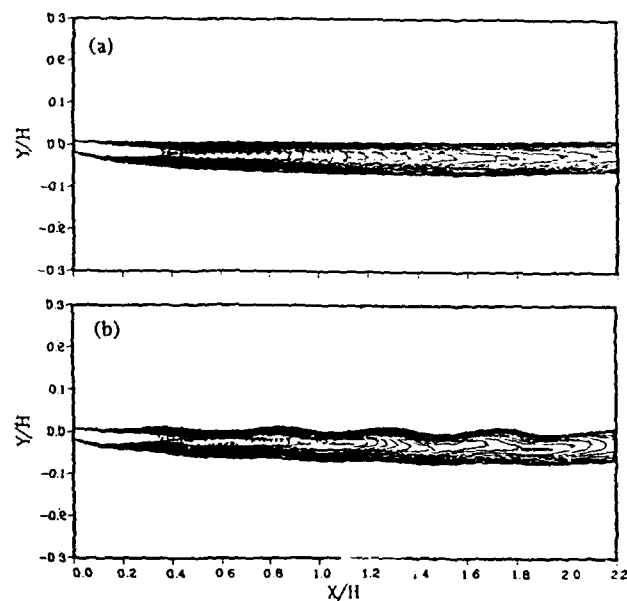


Figure 5. Vorticity contours for case-4, $M_1=5.0$, $M_2=1.3$, $Mc=1.2$.
(a) without disturbance. (b) with disturbance in the normal direction.

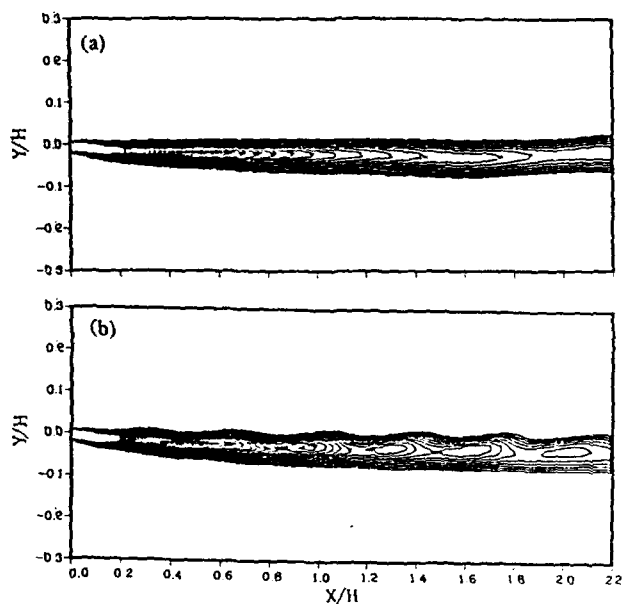


Figure 4. Vorticity contours for case-3, $M_1=4.0$, $M_2=1.3$, $Mc=0.8$.
(a) without disturbance. (b) with disturbance in the normal direction.

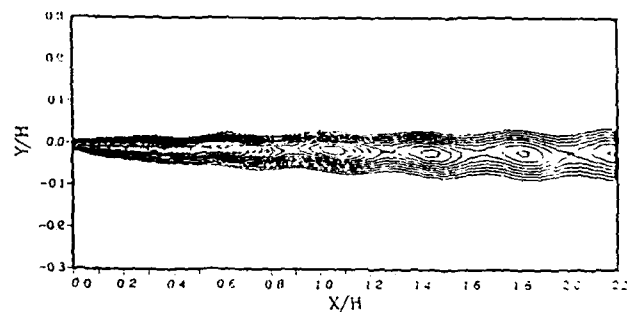


Figure 6. Effect of streamwise disturbances for Case 1.

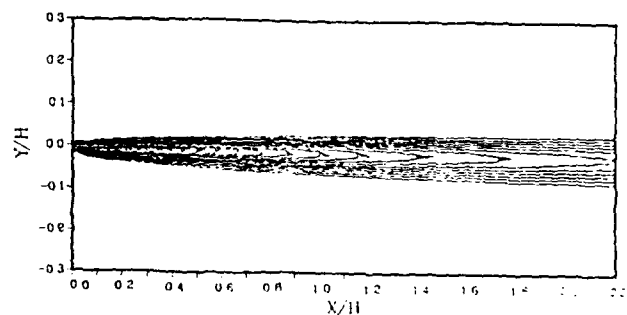


Figure 7. Effect of spanwise disturbances for Case 1.

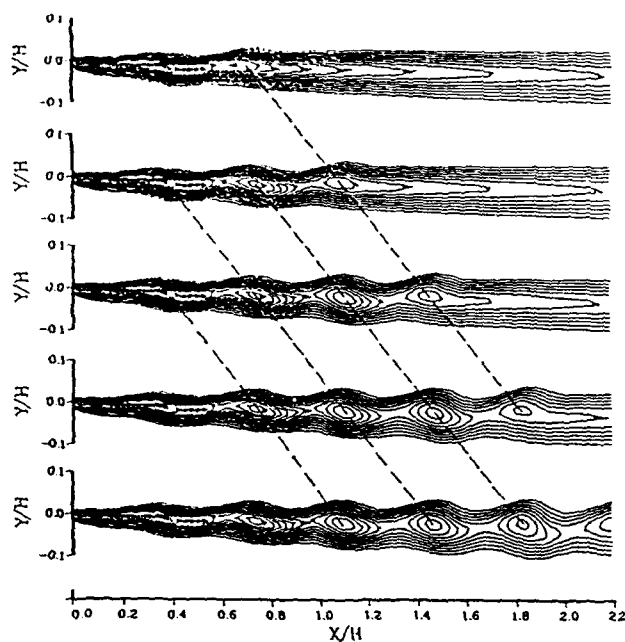


Figure 8. Computation of convective speed based on the temporal evolution of vorticity contours for Case 2.

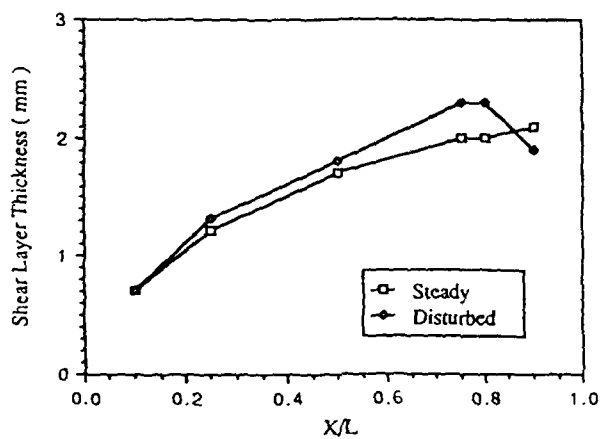


Figure 9. Shear layer thickness.

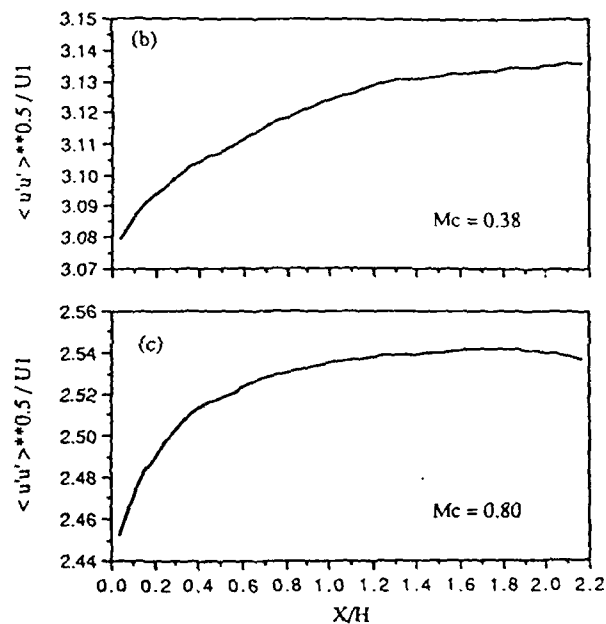
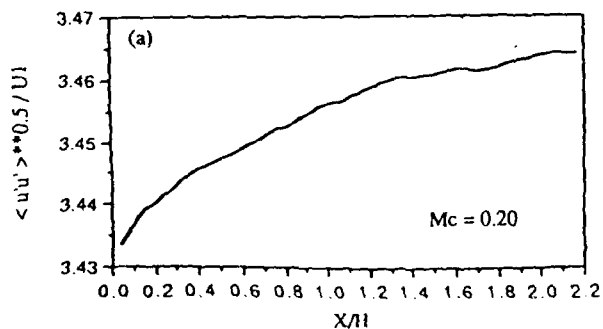


Figure 10. Effect of convective Mach number on fluctuation in the shear layer.
(a) $Mc=0.20$; (b) $Mc=0.38$; (c) $Mc=0.80$.

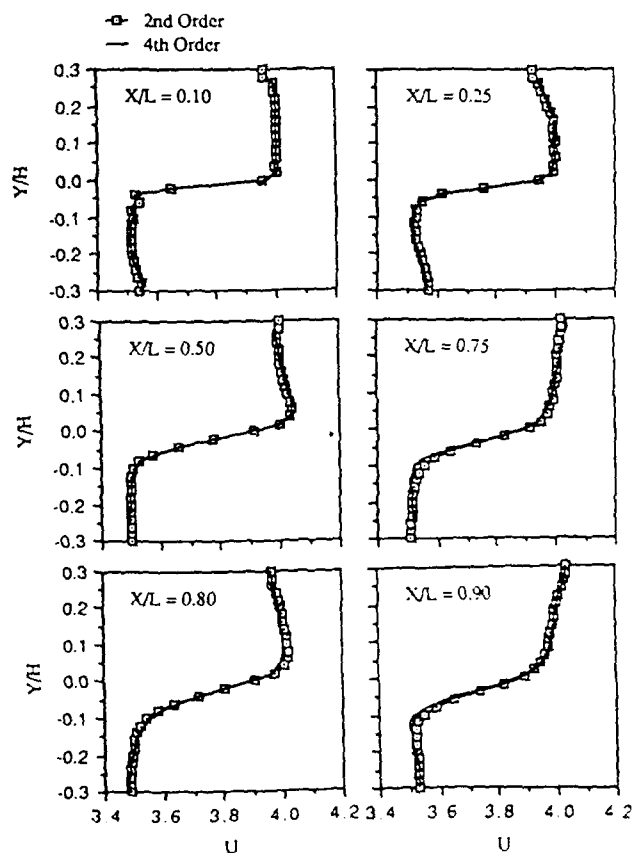


Figure 11. Velocity profiles across the shear layer: comparison of second and fourth order MacCormack schemes for case-1 with 111x31 grid.

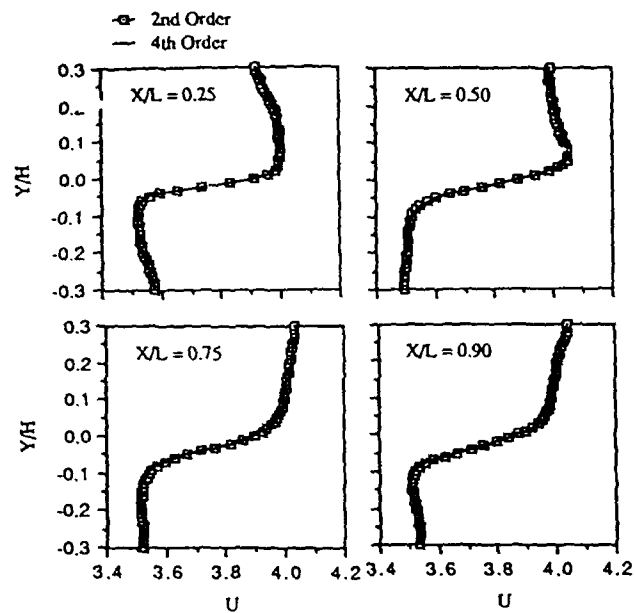


Figure 12. Velocity profiles across the shear layer: comparison of second and fourth order MacCormack schemes for case-1 with 221x61 grid.

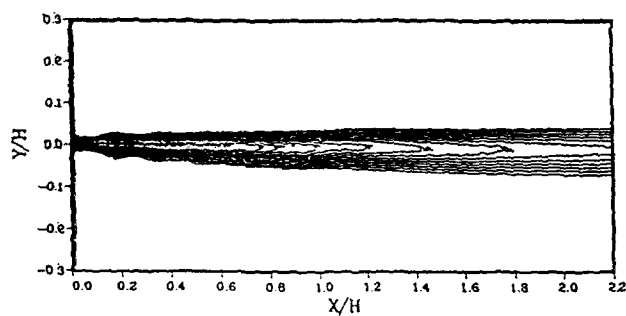


Figure 13. Vorticity contours obtained from ADI scheme for case-1 with disturbance.

AIAA '89

AIAA 89-0981

MIXING ENHANCEMENT IN SUPERSONIC FREE SHEAR LAYERS

W. Tang, L. N. Sankar and N. Komerath
School of Aerospace Engineering
Georgia Institute of Technology, Atlanta, GA 30332

AIAA 2nd Shear Flow Conference

March 13-16, 1989 / Tempe, AZ



For permission to copy or republish, contact the American Institute of Aeronautics and Astronautics
370 L'Enfant Promenade, S.W., Washington, D.C. 20024

MIXING ENHANCEMENT IN SUPERSONIC FREE SHEAR LAYERS

W. Tang¹, L. N. Sankar² and N. Komerath³School of Aerospace Engineering
Georgia Institute of Technology, Atlanta GA 30332

ABSTRACT

The issue of enhancing mixing between parallel, supersonic streams is numerically investigated. An explicit time marching scheme that is second order accurate in time and fourth order accurate in space is used to study this problem. Small amplitude velocity disturbances at selected frequencies are imposed over an otherwise steady flow at the juncture of the two streams to promote mixing. It is found that disturbances are selectively amplified at certain frequencies, while disturbances at other frequencies are rapidly damped out. In studies where the relative Mach number of the disturbances relative to one of the streams is high, shocklets were found to form on one or both sides of the shear layers. In such a situation, the relative Mach numbers of the eddies were different in coordinate systems attached to the upper and the lower streams.

INTRODUCTION

Aircraft engine and missile manufacturers are presently interested in a class of propulsion systems called SCRAMJET engines. In these systems the supersonic airstream captured at the inlet is slowed down to modest supersonic speeds through a series of shock waves prior to entering the combustion chamber. Here the airstream is allowed to mix and react with a parallel stream of fuel or partially burnt fuel/air mixture. For efficient performance of these systems, it is necessary that the fuel and air streams mix with each other as rapidly as possible, over a fairly short distance.

Unfortunately, supersonic free shear layers which form at the juncture of the air and fuel streams tends to grow very slowly [Ref. 1-3] compared to their subsonic counterparts. Alternate mechanisms such as normal injection of fuel into the airstream will likely increase mixing, but at the expense of significant total pressure losses.

Therefore, there is some interest in the use of active and passive control techniques which will promote mixing.

PREVIOUS WORK

A comprehensive discussion of recent experimental, numerical and analytical studies on the behavior of subsonic and supersonic shear layers has been done by Dimotakis [Ref. 4]. Here, only a small subset of existing work, closely related to the present numerical studies, is reviewed.

Experimental Studies: Chinzei et al. [Ref.1] have experimentally studied the growth rate of planar shear layers, using Schlieren techniques, and total pressure probes. They found organized vortical structures to exist in such flows, in a manner similar to subsonic shear layers. Perhaps the best known experimental work on supersonic planar shear layers is that done by Papamoschou and Roshko [ref. 2,3], for a variety of gases and flow conditions on either side of the shear layer. They showed that the convective Mach number of the eddies is a significant parameter governing the growth rate of supersonic shear layers. Papamoschou also performed stability analyses of infinitely thin shear layers (vortex sheets) to link the growth rate of the shear layer (compared to that of an incompressible shear layer) to the convective Mach number, and derived closed form expressions for the convective Mach number as a function of flow conditions on either side. The idea of convective Mach number itself is, of course, not new, and has been previously derived by Bogdanoff [Ref. 5]. In a later study [Ref. 6], Papamoschou found that the measured convective Mach number of the eddies matches the analytical predictions only when the convective Mach number is low and subsonic. He attributed this discrepancy to the fact that the traditional derivations for the convective Mach number assume the total pressure on either side of the shear layer to be equal. In cases where the convective Mach number is high, shocklets can form and lead to different amounts of total pressure losses on either side of the shear layer. Papamoschou also studied modifications to the trailing edge of the splitter plate which initially

1. Research Engineer, Member AIAA.

2. Associate Professor, Member AIAA.

3. Assistant Professor, Member AIAA.

Copyright © 1989 by L. N. Sankar. Published by the American Institute of Aeronautics and Astronautics, Inc. with Permission.

separates the two streams to passively enhance the mixing rate, but found these modifications to be of little benefit.

Stability Analyses: The stability of free shear layers has been extensively studied in the past by a number of researchers [e.g. Ref. 7]. Perhaps because the role convective Mach number plays in the stability and growth characteristics had not been discovered at that time, many of these earlier works dealt with parametric studies where one or more of the flow parameters were varied in a systematic manner. During the past few years, Ragab and Wu [Ref. 8,9] have studied the stability characteristics of both planar and oblique disturbances in wakes and planar shear layers, and have studied the effects of convective Mach number, and the disturbance propagation angle on the shear layer stability. They found non-parallel flow effects to have a negligible effect on the stability characteristics. Recently, these investigators [Ref. 14] studied the effects of subharmonic waves in 2-D spatially periodic shear layers through a Floquet analysis [Ref. 10].

The effects of side walls on the stability characteristics of confined, planar shear layers were studied by Tam [Ref. 11]. For eddies travelling at supersonic (relative) speeds, these investigators pointed out that the acoustic waves propagating off these eddies may be reflected by the wall and interact with the shear layer leading to new modes of instabilities.

Recently, Sandham et al. [Ref. 12] and other researchers have carried out stability analyses of free and confined shear layers, using methods similar to that employed in the works mentioned above.

Direct Numerical Simulations: The behavior of supersonic free shear layers through a numerical solution of the unsteady compressible Navier-Stokes equations is now possible, thanks to the recent advancements in high order accuracy schemes, high speed computers and interactive graphics tools. Lele [Ref. 13,14] has developed spatially fourth order and sixth order accurate finite difference schemes to study temporally and spatially growing shear layers. When the shear layer is excited at the most unstable frequency of the shear layer, and at a subharmonic, his solutions

demonstrated features such as vortex pairing, shear layer roll up and formation of shocklets at high enough convective Mach numbers. The temporal growth of inviscid shear layers was studied by Soetrisno et al. [Ref. 15,16]. When the shear layer was initially seeded with disturbances at the most unstable frequency and a subharmonic, these investigators demonstrated that vortex roll up can occur, and that the total turbulent kinetic energy within the entire domain, grew very slowly at high convective Mach numbers. Their calculations showed evidence of weak shocklets in some cases.

The present investigators used a Fourth order MacCormack scheme to study temporal and spatial growth of thin shear layers, at very early stages of laminar mixing [Ref. 17,18], and studied the effects of convective Mach number as well as streamwise, spanwise and normal velocity disturbances on the shear layer growth. It was demonstrated that the growth rate of the shear layer decreased with increasing convective Mach number. In addition, the studies in Ref. 17 and 18 found the eddy speeds to be significantly different from Papamoschou's formulas for high convective Mach numbers.

Other passive and active control techniques for enhancing mixing between fuel and airstreams have also been studied. Guirguis [Ref. 19] suggested an arrangement where a bluff body is placed at the base of the splitter plate separating the air and fuel streams. Drummond and Mukunda [Ref. 20], and Kumar et al. [Ref. 21] have discussed a passive control technique where a system of stationary shock waves are used to generate vorticity in the flow. This vorticity interacts with the shear layer and leads to an increase in the turbulence level, and improved mixing of the shear layer.

OBJECTIVES OF THE PRESENT WORK

The objectives of the present work are to study the behavior of supersonic free shear layers at two extremes: a) at very low convective Mach numbers ($Mc < 0.2$) and (b) at very high convective Mach numbers ($Mc > 1$) relative to one of the two streams.

In order to understand the behavior of supersonic free shear layers at low convective Mach numbers, we investigate its response to arbitrary, user-specified acoustic disturbances over a broad range of frequencies. Sinusoidally varying velocity disturbances at a number of frequencies are introduced at the initial, laminar mixing region of the shear layer. These disturbances grow with time as they are convected downstream and eventually lead to well organized vortical structures. The objective of this work is then to study how the disturbances over the entire spectrum of frequencies behave as they are convected downstream, and to speculate on mechanisms by which energy is transferred from high frequencies to low frequencies and vice versa.

To study behavior of the shear layer at very high convective Mach numbers, we use vorticity and pressure contour plots at a number of time levels to track the velocity of the dominant eddies and compute the relative Mach number of these eddies in a coordinate system attached to either the faster stream or the slower stream. If supercritical Mach numbers arise relative to either stream, then the resultant pressure field is examined for the occurrence of shock waves, expansion waves and their effects on the shear layer growth.

The 2-D compressible Navier-Stokes equations in a strong conservation form are numerically solved, using a modified MacCormack scheme that is second order accurate in time, and fourth order accurate in space. This scheme is suitable for studying phenomena such as propagation of acoustic waves, boundary layer instability, and shear layer instability and has been previously used by several authors [Ref. 22-24]. The flow field is assumed to be laminar.

NUMERICAL FORMULATION

The 2-D, laminar, unsteady, compressible flow is governed by the Navier-Stokes equations which may be formally written as:

$$q_t + F_x + G_y = R_x + S_y$$

where F and G are inviscid flux terms, while R and S are the viscous stress terms.

In this work the above equation was solved using a splitting approach. That is, the solution was advanced from one time level 'n' to the next (n+2) through the following sequence of operations:

$$q^{n+2} = L_x L_y L_{xv} L_{yv} L_{yv} L_{xv} L_y L_x q^n$$

where, for example, the L_x operator involves solution of the following 1-D equation:

$$q_t + F_x = 0$$

This 1-D equation was solved through the following predictor-corrector sequence, recommended by Bayliss et al [Ref.22]:

Predictor Step:

$$q_i^* = q_i^n \Delta t / (6\Delta x) [7 F_i - 8 F_{i-1} + F_{i-2}]^n$$

Corrector Step:

$$q_i^{n+1} = (q_i^* + q_i^n) / 2 + \Delta t / (12\Delta x) [7 F_i - 8 F_{i+1} + F_{i+2}]^*$$

In the above equations, the j -index has been suppressed for clarity.

When the above equation is applied at nodes close to the left and right side boundary, a fourth order accurate extrapolation procedure was used to extrapolate the flux vectors F and G needed at nodes outside the computational domain.

The L_y operator requires solution of the equation

$$q_t + G_y = 0$$

using a similar approach.

The operators L_{xv} and L_{yv} correspond to numerical solution of 1-D equations such as

$$q_t - R_x = 0$$

The above equation was solved through the following two-step sequence:

$$q_i^* = q_i^n + \Delta t / \Delta x [R_{i+1/2} - R_{i-1/2}]^n$$

$$q_i^{n+1} = (q_i^n + q_i^*) / 2 + \Delta t / (2\Delta x) [R_{i+1/2} - R_{i-1/2}]^*$$

The viscous terms are thus updated only to second order accuracy in space.

It may be shown that the above scheme has very little artificial dissipation inherent in it, and is fourth order accurate in space, as far as the inviscid part is concerned. In high Mach number streams, it is anticipated that the symmetric nature of the above scheme may cause inappropriate transfer of information from the downstream nodes to the upstream. To prevent this, three-point upwind schemes are also available as an option in the computer code, which use expressions such as

$$F_x = (3 F_i - 4 F_{i-1} + F_{i-2}) / 2\Delta x$$

during both the predictor and corrector stages of the solution. All the results to be presented here were carried out using the fourth order accurate symmetric form.

RESULTS AND DISCUSSION

Figure 1 shows the computational domain used. In the discussions that follow, all velocities have been normalized by the velocity of the faster stream; all temperatures and densities have likewise been normalized the corresponding values of the faster stream. The distances have been normalized by the vorticity thickness of the prescribed mean velocity profile at the upstream boundary.

The computational domain was divided into a uniformly spaced Cartesian grid consisting of 221 nodes in the x- direction and 241 nodes in the normal direction. The typical grid spacing in the x- and y- direction were $5/3\delta$ and 0.4δ units respectively, where δ is the vorticity thickness of the shear layer at the inflow boundary, as discussed earlier. The grid spacing in the y- direction is fine enough to place approximately 30 points across the shear layer where the vorticity content is largest, at

distances sufficiently downstream ($x > 50\delta$) from the inlet.

As stated earlier, the objectives of the present work are to study shear layer characteristics at low and high convective Mach numbers. The method employed is the same. The shear layer is subjected to arbitrary, user input disturbances. The resulting velocity, vorticity and pressure fields are studied to gain an understanding of the shear layer behavior.

1. Shear Layer Behavior at Subsonic Convective Mach Numbers:

The initial and boundary conditions for this study are as follows. At the inflow boundary, the following mean velocity profile was specified:

$$U_{\text{mean}}(y) = (U_1 + U_2) / 2 + (U_1 - U_2) / 2 \tanh(y/\delta)$$

Here U_1 and U_2 are the velocities on either side of the shear layer at sufficiently large distances away from the shear layer, and are equal to 1.0 and 0.25 respectively. Also, δ is the vorticity thickness at the inflow, equal to unity. The v component of inflow velocity was set to zero for the mean flow. The pressure was assumed to be equal and uniform at the inflow boundary. The density and temperature ratios were as follows:

$$T_1 = 1.0 ; T_2 = 0.65 ; \rho_1 = 1.0 ; \rho_2 = 1.535$$

The Reynolds number of the flow, defined as $U_1 \delta \rho_1 / \mu_1$ was of the order of 25. The convective Mach number for this particular flow combination was 0.2. One can compute the convective Mach number by tracking vortices as they are convected downstream, as discussed in Ref. 18. Alternatively, one can compute the convective Mach number using Papamoschou's formula [Ref. 2]. In this particular case, these approaches agree to within 3%.

At the top and bottom boundaries the flow may be either confined, or free. If the flow is confined, then the normal velocity at these boundaries was set to zero. The density and temperature at these boundaries were evaluated using the zero gradient condition. The x- component of velocity at this boundary was also extrapolated using a zero gradient condition. This is

equivalent to applying a slip boundary condition at these walls. In the case of free, unconfined shear layers, non-reflective boundary conditions are needed at these lateral boundaries. In the present work, setting the derivative of the normal component of velocity to zero, rather than the velocity itself to zero was found to minimize reflections.

The flow properties at the inflow were specified everywhere in the flow field as the initial conditions for the problem. The Navier-Stokes solver was then advanced for several non-dimensional units of time, until a fully developed shear layer with a modest streamwise growth was established.

Once a steady state shear flow was achieved, forced excitation of the shear layer began. This was achieved by prescribing the normal (v -) component of velocity over the entire inflow boundary to behave as follows:

$$v(y, x=0, t) = \sum A_n f(y) \sin(\omega_n t + \theta_n)$$

Here the summation shown is over all the excitation frequencies; A_n is the amplitude of disturbance, ω_n is the frequency of disturbance and θ_n is the associated phase angle. The function $f(y)$ determines the variation of the perturbation velocity across the shear layer. Both a Gaussian distribution and a constant magnitude distribution were attempted. The results to be presented here correspond to $f(y)$ equal to unity.

In the present work 6 frequencies were used, with zero phase difference between the individual components. The quantity A_n was 2% of the reference velocity U_1 . The non-dimensional frequencies ω_n were 10, 20, 30, 40, 50 and 60 respectively. Obviously, a linear stability analysis could have been used to pick the frequencies that are related to the most unstable frequency. But the intent here was to impose excitation at several frequencies on the shear layer, at the inflow boundary and determine which frequencies are selectively amplified, and to determine what happens to the energy content at the higher frequencies at subsequent time levels.

Figure 2 shows the vorticity contours at a randomly selected time level. It is seen that the

vorticity field at the immediate downstream boundary is rich in structure showing large gradients in the streamwise as well as normal directions. At large distances downstream, however, only a single row of eddies at well defined distances are seen.

Because the formation and motion of vortices (or eddies) give rise to a rapidly varying pressure field which moves with the eddies some useful information about the energy content at the shear layer distributed over the various frequencies may be obtained by computing the Fourier transform of the pressure field at a number of points within the shear layer. In figure 3, the Fourier spectrum of the pressure field is plotted at 6 x -locations within the computational field, at $y/\delta = 0$. The following trend is seen. Near the inflow boundary, the Fourier spectrum shows a near uniform distribution over the entire frequency range. At downstream locations, the higher frequency content begins to gradually decrease. The low frequency components at non-dimensional frequencies 10 and 20 show a rapid increase initially, but reaches asymptotically constant values. Figure 4 contains the same information as figure 3, except it shows the changes in energy content as a function of downstream distance. It is seen that Fourier coefficient associated with non-dimensional frequency 60 reduces to 30% of initial value 100 δ downstream, whereas the low frequency component triples in magnitude and reaches its limit value 125 units downstream. An examination of the vorticity contour plot (figure 2) shows a number of small eddies at the inflow boundary, which rapidly merge into a single, large vortex. This merging appears to be the mechanism responsible for the decrease in the energy content at high frequencies, and the corresponding increase at the lower frequencies. It is interesting to note that the two lowest frequency components (corresponding to non-dimensional frequencies 10 and 20) maintain their energy levels once they reach their limit values, with no further transfer of energy from the $\omega_n = 20$ waves to the $\omega_n = 10$ waves. This may be due to the fact that the phase difference in the forcing function corresponding to these two waves was zero.

II. Behavior of Supersonic Shear Layers at High Convective Mach Numbers:

In his early work on supersonic free shear layers, Papamoschou [Ref. 2] derived an expression for the convective Mach number and suggested that the convective Mach number of the eddy relative to the faster stream is the same as the convective Mach number of the slower stream relative to the eddy. That is, if U_c is the velocity of the eddy, then

$$(U_1 - U_c) / a_1 = (U_c - U_2) / a_2$$

when the gases above and below have the same ratio of specific heat.

In subsequent experimental studies, Papamoschou found that the above relation did not hold true when the convective Mach number on either side of the eddy rose high enough to give shock waves. The eddy appeared to be dragged along with either the faster scheme or the slower stream, and the convective Mach numbers of the eddy relative to the stream above and below were not equal.

Dimotakis [Ref.4] has discussed on the probable causes of this phenomenon and suggests that there may be unequal total pressure losses on either side of the eddy, due to the occurrence of shock waves. He further discusses situations where the convective Mach number relative to one of the two streams can become very low, and the convective Mach number relative to the second stream can become very high, leading to shocklets only on one side of the shear layer. A hysteresis phenomenon, where shocklets appear alternatively on either side of the shear layer is also possible, according to Dimotakis.

In an earlier study, the present investigators computed the convective Mach number of eddies arising in the early stages of mixing of a laminar shear layer. It was found that at high enough convective Mach numbers the eddies appeared to travel at a speed closer to the faster stream, and was "dragged along" by the faster stream. The present study is an attempt to study the pressure fields and shocklets that arise when the convective Mach number relative to the faster and slower

streams is high. Three cases have been studied, which are discussed below.

Case 1: The flow conditions were:

$$M_1 = 6.0 ; M_2 = 3.6 ; T_2/T_1 = 1.0 ; P_2 = P_1$$

The velocity profile was given by a Tanh profile, similar to that used for the subsonic case discussed earlier.

At the inflow boundary, a sinusoidally varying normal velocity disturbance was introduced at a single non-dimensional frequency, 60. The resulting velocity fields and vorticity fields were analyzed after several cycles of forced response of the shear layer. When the trajectories of these eddies were analyzed in the x-t frame, it was found that the eddies in the shear layer initially accelerate, until they reach a convective Mach number relative to the faster stream approximately equal to 0.5. Papamoschou's formula for this case yields a convective Mach number of 1.2. Thus the numerical predictions of the present code and Papamoschou's formula are in significant disagreement. The relative Mach number between the eddy and the lower stream are found to be well in excess of unity (approximately 1.9).

When the pressure field is plotted at a randomly chosen time level, the following features are observed (Figure 6). The relative Mach numbers with respect to both the upper and lower streams are initially high enough, and give rise to shocklets as shown in figure 6. In figure 6, the dotted contours correspond to high pressure levels, while the solid lines correspond to lower pressures. The vorticity plot (shown in figure 5) is also seen to show closed vorticity contours approximately aligned with the shocks, just behind the shocklets. An inspection of the pressure jumps across the shocklets indicates that the shocklets on the lower side appear to be stronger than those on the upper side, as expected.

Case 2: The flow conditions for this case were:

$$M_1 = 5.0 ; M_2 = 1.3 ; T_1 = 1.53 T_2, P_1 = P_2$$

As in the earlier cases, a tanh profile was used, and single frequency normal velocity excitations were introduced at the inflow boundary.

In figures 7 and 8, the pressure and velocity contours are plotted at a randomly chosen time level. In this case, from an inspection of the vorticity profiles at adjacent time levels, the eddies appear to travel at substantially lower speed than the upper stream. During the early stages of eddy formation and motion, shocklets occur both on the upper and lower sides of the shear layer. As the eddies accelerate and reach low subsonic Mach numbers relative to the upper stream, the shocklets on the upper side of the shear layer disappear. The shocklets on the lower side continue to travel with the eddies, with no reduction in their strength.

Case 3: Case 1 was repeated, by artificially reducing the shear layer vorticity thickness by a factor of 15, keeping all other dimensions such as the grid size, domain length and width constant. In figures 9 and 10, the pressure and vorticity contours are plotted. Again, in figure 10, the solid and dotted contours correspond to low and high pressure levels respectively. Shocklets are evident on either side of the shear layer, although they are weak because the reduced shear layer thickness leads to small and thin eddies, compared to case 1.

Case 4: As a final exercise, Case 1 was repeated, with forced excitation of the normal velocity at the inflow boundary over multiple frequencies, ranging from 10 to 60. The amplitude of the individual components was 0.02 times the upperstream velocity. In figure 11 the Fourier spectrum of the pressure field at several x- locations are plotted. A gradual migration of energy levels from the higher frequency to the lower frequencies is evident, as in the case of the subsonic convective Mach number case. Figure 12 shows how the two high frequency components decay following a brief initial growth as eddies are convected downstream. The low frequency components at frequencies 10, 20 and 30 initially grow rapidly, but reach asymptotic values.

The response of the shear layer to multiple frequencies is strikingly similar to that in the earlier study for subsonic convective Mach numbers, shown in figures 3 and 4.

CONCLUDING REMARKS

The stability and growth characteristics of supersonic free shear layers were studied by

exciting the shear layer at the upstream boundary with small amplitude normal velocity disturbances. The following observations were made:

a) In the case of shear layers at subsonic and supersonic convective Mach numbers, the imposition of acoustic disturbances over a large range of frequencies lead to the transfer of this energy from the high frequencies to the low frequencies, as the flow progressed from the upstream boundary to the downstream boundary. The energy content at the lowermost frequencies rapidly reached asymptotic values following which eddies in the shear layer were convected downstream with no further alteration in their structure.

b) In the case of shear layers at a supersonic convective Mach number, situations were found where the convective Mach number relative to the faster stream is low. This leads to a situation where shocklets arose only on the lower side of the shear layer. Conditions were also found where the convective Mach number relative to both the streams is high, leading to shocklets on either side. These calculations demonstrate the same features experimentally observed by Papamoschou [Ref. 3] and discussed based on total pressure arguments by Dimotakis [Ref 4].

ACKNOWLEDGEMENTS

This work was supported by the Office of Naval Research under Grant No. N00014-89-J-1319. Computer time for the numerical simulations was provided by the Pittsburgh Supercomputing Center. The authors are thankful to Prof. S. A. Ragab of Virginia Polytechnic Institute & State University for several valuable discussions.

REFERENCES

1. Chinzei, N., Masuya, G., Komuro, T., Murakami, A. and Kudou, K., "Spreading of Two-Dimensional Supersonic Mixing Layers," *Physics of Fluids*, Vol. 29, pp1345-1347.
2. Papamoschou, D., "Experimental Investigation of Heterogeneous Compressible Shear Layers," Ph. D. Dissertation, Cal Tech, 1986.

3. Papamoschou, D. and Roshko, A., "Observations on Supersonic Free Shear Layers," AIAA Paper 86-0162, January 1986.
4. Dimotakis, P., "Turbulent Free Shear Layer Mixing," AIAA Paper 89-0262, January 1989.
5. Bogdanoff, D.W., "Compressibility Effects in Turbulent Shear Layers," AIAA Journal, Vol. 21, No. 6, 1983, pp926-927.
6. Papamoschou, D., "Structure of the Compressible Shear Layer," AIAA 89-0126, January 1989.
7. Lessen, M., Fox, J. and Zien, H. M., "On the Inviscid Stability of the Laminar Mixing of Two Parallel Streams of a Compressible Fluid," Journal of Fluid Mechanics, Vol. 23, part 2, pp355-367, 1965.
8. Ragab, S. A. and Wu, J. L., "Instabilities in the Free Shear Layer Formed by Two Supersonic Streams," AIAA Paper 88-0038, 1988.
9. Ragab, S., "Instabilities in the Wake/Mixing Layer Region of a Splitter Plate Separating Two Supersonic Streams," AIAA Paper 88-3677-CP, 1988.
10. Ragab, S. and Wu, J. L., "Linear Subharmonic Instabilities of Periodic Compressible Mixing Layers," AIAA Paper 89-0039, January 1989.
11. Tam, C.K.W. and Hu, F. Q., "Instabilities of Supersonic Mixing Layers Inside a Rectangular Channel," Proceedings of the First National Fluid Dynamics Congress, July 1988.
12. Sandham, N. and Reynolds, W., "The Compressible Mixing Layer: Linear Theory and Direct Simulation," AIAA Paper 89-0371, January 1989.
13. Lele, S., "Vortex Evolution in Compressible Free Shear Layers," Workshop on the Physics of Compressible Turbulence, October 1988.
14. Lele, S., "Direct Numerical Simulation of Compressible Free Shear Flows," AIAA Paper 89-0374, January 1989.
15. Soestrisno, M., Eberhardt, S., Riley, J. and McMurtry, P., "A Study of Supersonic Mixing Layers Using a Second Order TVD Scheme," AIAA Paper 88-3676-CP.
16. Greenbough, J., Riley, J., Soestrisno, M. and Eberhardt, D., "The Effects of Walls on a Compressible Mixing Layer," AIAA Paper 89-0372, January 1989.
17. Sankar, L. N., Tang, W. and Komerath, N., "Navier-Stokes Simulation of Supersonic Free Shear Layers," Physics of Compressible Turbulent Mixing Workshop, Princeton University, October 24-27, 1988.
18. Tang, W., Komerath, N. and Sankar, L. N., "Numerical Simulation of the Growth of Instabilities in Supersonic Free Shear Layers," AIAA Paper 89-0376, 1989.
19. Guirguis, R. H., "Mixing Enhancement in Supersonic Shear Layers: III. Effect of Convective Mach number," AIAA 88-0701.
20. Drummond, J. P. and Mukunda, H. S., "A Numerical Study of Mixing Enhancement in Supersonic Reacting Flow Fields," AIAA Paper 88-3260.
21. Kumar, A., Bushnell, D. M. and Hussaini, M. Y., "A mixing Augmentation Technique for Hypervelocity Scramjets," AIAA Paper 87-1182.
22. Bayliss, A., Maestrello, L., Parikh, P. and Turkel, E., "Numerical Simulation of Boundary Layer Excitation by Surface Heating and Cooling," AIAA Journal, Vol. 24, No. 7, July 1986.
23. Bayliss, A. and Maestrello, L., "Simulation of Instabilities and Sound Radiation in a Jet," AIAA Journal, Vol. 9, No. 7, July 1981.
24. Hariharan, S. and Lester, H., "A Finite Difference Solution for the Propagation of Sound in Near Sonic Flows," NASA TM 84663, July 1983.

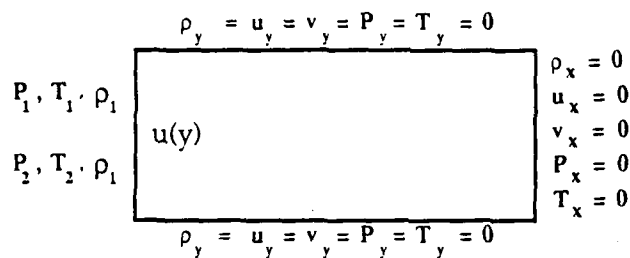


Figure 1. Computational domain

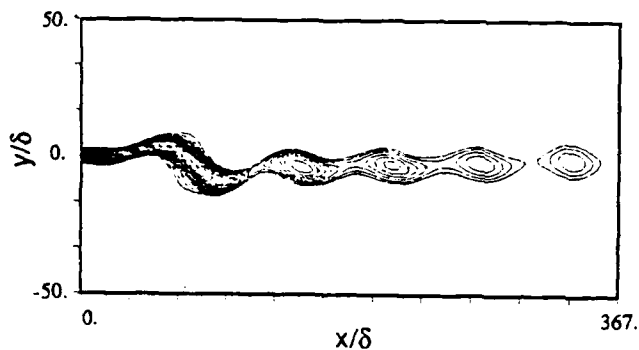


Figure 2. Vorticity Contours for a shear layer excited at multiple frequencies; $Mc=0.2$, $M_1=4.0$, $M_2=2.3$, $a_1/a_2=2.3$, $\delta=1/15$.

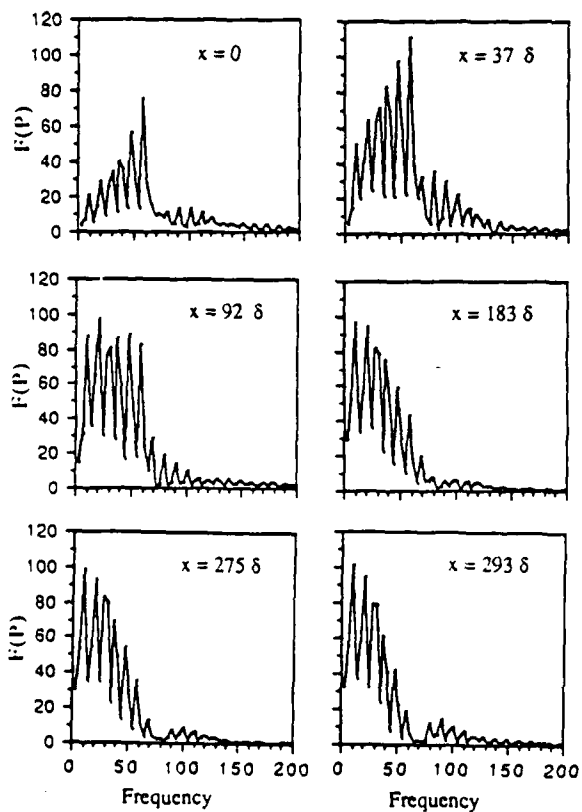


Figure 3. Fourier spectrum of pressure field at selected x-locations within the shear layer; $Mc=0.2$, $M_1=4.0$, $M_2=2.3$, $a_1/a_2=2.3$, $\delta=1/15$.

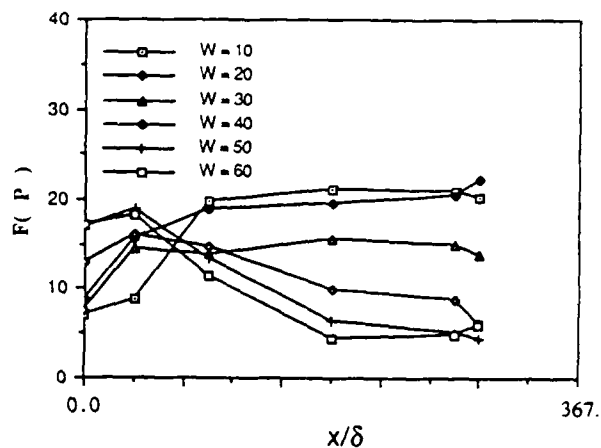
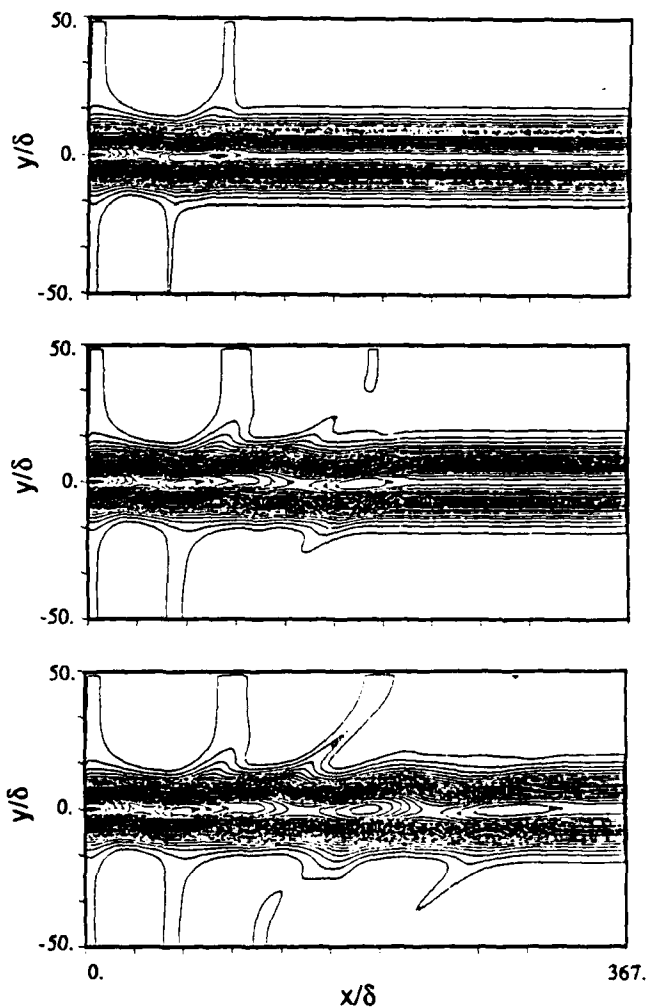


Figure 4. Variation of Fourier spectrum as a function of streamwise location; $Mc=0.2$, $M_1=4.0$, $M_2=2.3$, $a_1/a_2=2.3$, $\delta=1/15$.



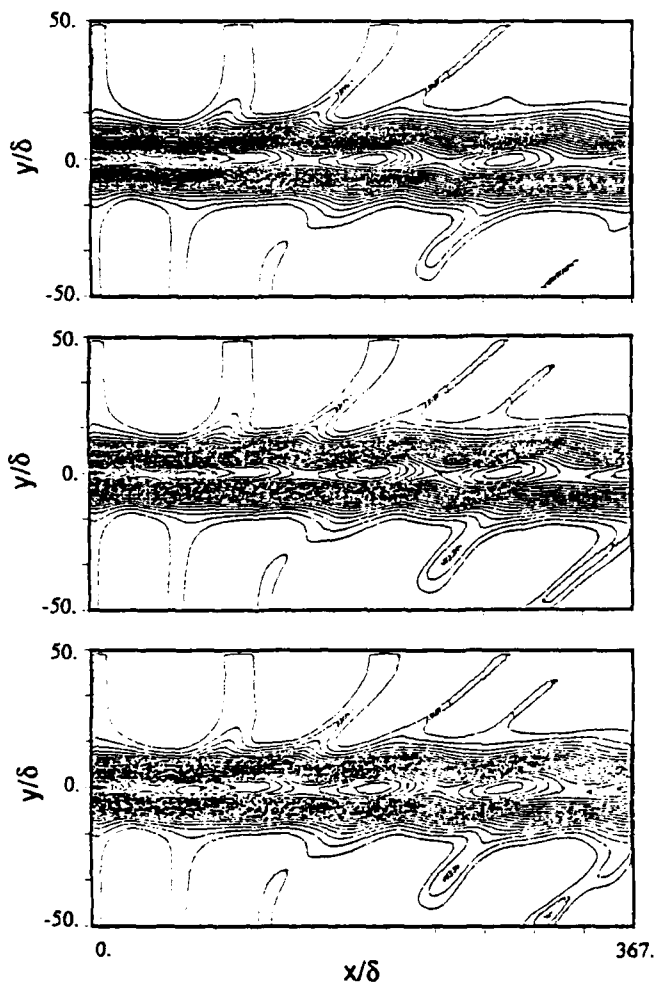


Figure 5. Vorticity contours at selected time levels for a shear layer excited at a single frequency; $Mc=1.2$, $M_1=6.0$, $M_2=3.6$, $a_1/a_2=1.0$, $\delta=1.0$.

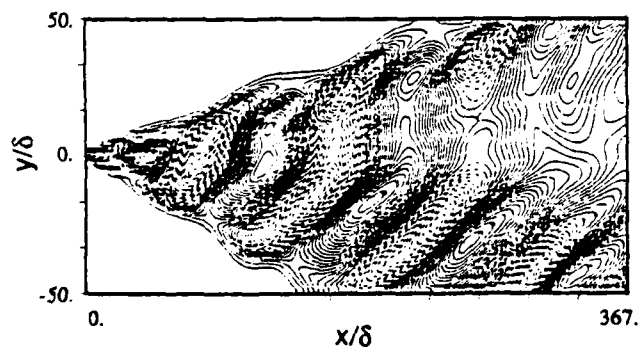


Figure 6. Typical pressure contours for conditions of Figure 5.

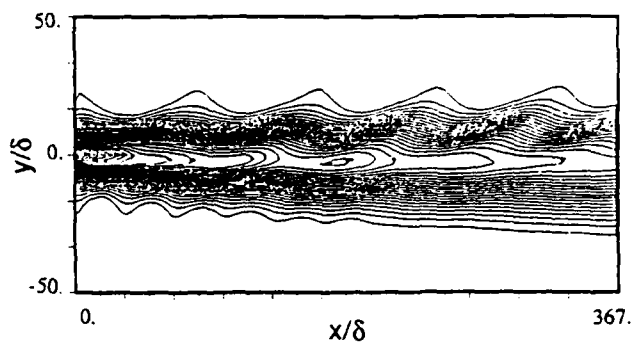


Figure 7. Typical vorticity contours for $Mc=1.2$, $M_1=5.0$, $M_2=1.3$, $a_1/a_2=2.3$, $\delta=1.0$.

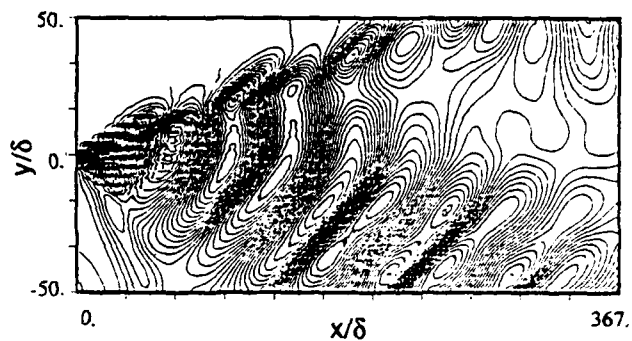


Figure 8. Typical pressure contours for $Mc=1.2$, $M_1=5.0$, $M_2=1.3$, $a_1/a_2=2.3$, $\delta=1.0$.

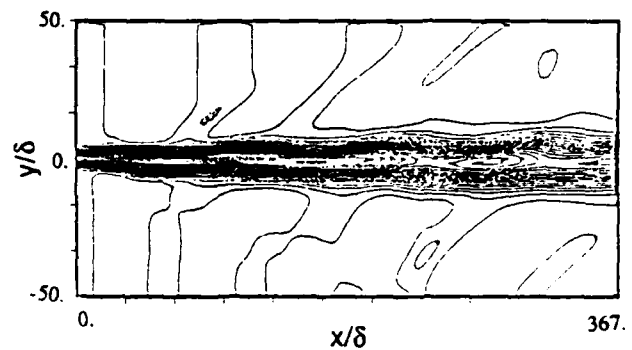


Figure 9. Typical vorticity contours for $Mc=1.2$, $M_1=6.0$, $M_2=3.6$, $a_1/a_2=1.0$, $\delta=1/15$.

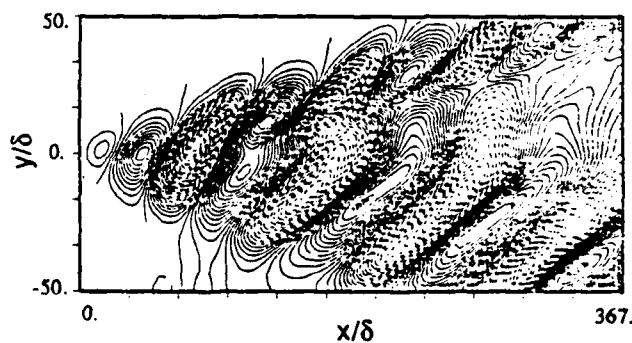


Figure 10. Typical pressure contours for $Mc=1.2$, $M_1=6.0$, $M_2=3.6$, $a_1/a_2=1.0$, $\delta=1/15$.

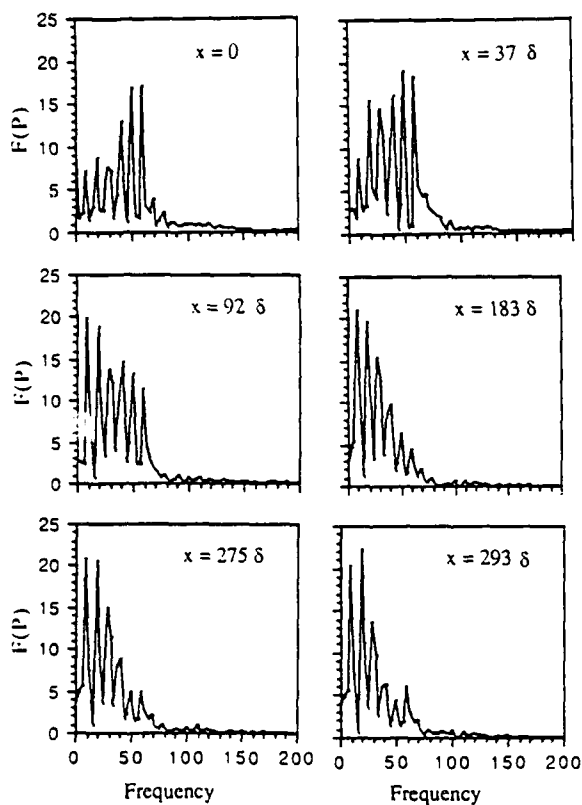


Figure 11. Fourier spectrum of pressure field at selected x -locations within the shear layer; $Mc=1.2$, $M_1=6.0$, $M_2=3.6$, $a_1/a_2=1.0$, $\delta=1/15$.

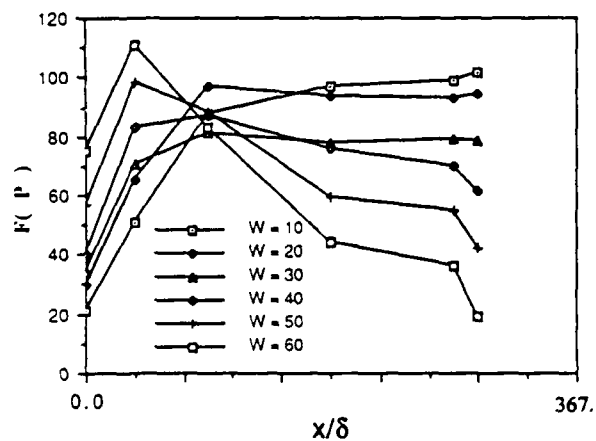


Figure 12. Variation of Fourier spectrum as a function of streamwise location; $Mc=1.2$, $M_1=6.0$, $M_2=3.6$, $a_1/a_2=1.0$, $\delta=1/15$.